

N-Phonon Bundle Emission via the Stokes Process

Qian Bin,¹ Xin-You Lü,^{1,*} Fabrice P. Laussy^{2,3}, Franco Nori,^{4,5} and Ying Wu^{1,†}

¹School of Physics, Huazhong University of Science and Technology, Wuhan, 430074, People's Republic of China

²Faculty of Science and Engineering, University of Wolverhampton, Wulfruna Street, Wolverhampton WV1 1LY, United Kingdom

³Russian Quantum Center, Novaya 100, 143025 Skolkovo, Moscow Region, Russia

⁴Theoretical Quantum Physics Laboratory, RIKEN Cluster for Pioneering Research, Wako-shi, Saitama 351-0198, Japan

⁵Physics Department, The University of Michigan, Ann Arbor, Michigan 48109-1040, USA



(Received 2 August 2019; accepted 8 January 2020; published 3 February 2020)

We demonstrate theoretically the bundle emission of n strongly correlated phonons in an acoustic cavity QED system. The mechanism relies on Stokes resonances that generate super-Rabi oscillations between states with a large difference in their number of excitations, which, combined with dissipation, transfer coherently pure n -phonon states outside of the cavity. This process works with close to perfect purity over a wide range of parameters and is tunable optically with well-resolved operation conditions. This broadens the realm of quantum phononics, with potential applications for on-chip quantum information processing, quantum metrology, and engineering of new types of quantum devices, such as optically heralded n -phonon guns.

DOI: 10.1103/PhysRevLett.124.053601

The manipulation of quantum states is one of the main topics of modern science. In the case of photons, an increasingly popular research line is that of multiphoton physics [1–6], with potential applications for multiphoton lasers [7], beating the diffraction limit [8], and metrology [9]. In particular, a scheme for the direct generation of n -photon states in the same mode (n -photon bundles) has been recently proposed under the platform of cavity quantum electrodynamics (cQED) [4].

Besides photons, phonons (the quanta of mechanical waves) have emerged as strong candidates for the engineering of solid-state quantum devices and on-chip quantum communications, with several distinct advantages. First, the speed of acoustic waves is significantly slower than the speed of light, and thus it is more suitable for communications over short distances, such as a few hundred micrometers or less (i.e., on-chip communication) [10,11]. Second, since phonons can only propagate in a medium, they are immune to radiation losses into the vacuum. Lastly, phonon cavities are greatly tunable, with resonant frequency-ranges from gigahertz (GHz) to terahertz (THz) having already been fabricated [12–19]. THz phonons have wavelengths comparable to the lattice constants, which have important applications for sensing and nanoscale imaging, such as detecting microscopic subsurface structures with atomic precision. Consequently, quantum phononics has progressed enormously, including the investigation of phonon lasers [20–22], phononic quantum networks [23,24], the detection of electron-phonon interaction in double quantum dots [25,26], and quantum acoustic devices [27,28]. The generation of multiphonon quantum states, as a fundamental milestone on the road of

acoustic quantum devices, becomes an important task of phononics. For example, antibunching bundles and NOON phonon states could be valuable as n -phonon sources [29,30] and for acoustic quantum precision measurements [31,32], respectively. Multiphonon processes have also important applications in ultrasensitive biodetection [33].

Here, we present a method for implementing n -phonon bundle emission from a quantum dot (QD) coupled to an acoustic nanocavity with electron-phonon coupling and coherently driven by a laser at the n th-order phonon sideband. This optically driven Stokes process realizes super-Rabi oscillations [34] between states with large differences in their number of excitations. The pure bundle emission can be achieved by opening a dissipative channel for such super-Rabi oscillations induced by the Stokes resonances. Compared to the earlier work on n -photon bundles emission [4], here we have a different physical mechanism for achieving super-Rabi oscillations, i.e., through the optically driven Stokes process. In particular, the QD flip is accompanied by an n -phonon generation in the cavity, induced by the electron-phonon interaction. In contrast, Ref. [4] relies on the excitation of a dressed QD at the $(n+1)$ th rung together with an n -quanta energy transfer from the QD to the cavity, induced by the Jaynes-Cummings interaction, i.e., Purcell enhancing the so-called leapfrog transitions. Our work introduces the nonlinear Stokes process into the theory of bundle emission. This enlarged regime together with the more complex level structure shows that n -quanta bundle emission is not limited to particular platforms and configurations but can be exploited in more general settings; in particular since the ideal Stokes resonance can be realized over a wide range of parameters.

The different mechanism leads to a series of exclusive advantages featured by our proposal. Our implementation is robust to varying electron-phonon coupling strengths and/or driving strengths, which only change the resonant conditions. This leaves much room to achieve n -phonon bundle emission and optimize its purity. We find close to 99% two-phonon emission and 97% three-phonon emission with today's figures of merit [12–15]. Moreover, here we have the mixed phonon-photon emission, which allows us to efficiently and conveniently isolate the useful strongly correlated n -phonon emission from the other (optical) deexcitation channels. This could be used for the realization of optical heralded n -phonon lasers and guns. Our work opens potential applications for on-chip quantum communications, e.g., transferring quantum information with bundles of phonons in future on-chip quantum networks [35,36]. It also provides the important family of nonlinear Stokes processes with a new type of quantum engineering, besides the widely applied photon and phonon manipulations, such as the generation of paired photons [37], electromagnetically induced transparency [38], sideband cooling of mechanical oscillators [39], etc., [40,41].

Model and Stokes resonance.—We consider a phonon cQED model, with a QD coupled to a single-phonon mode of an acoustic nanocavity with electron-phonon coupling λ , as shown in Fig. 1(a). The QD is a two-level system with conduction-band state $|c\rangle$, valence-band state $|v\rangle$, and band-gap frequency ω_σ . The QD is driven by an optical

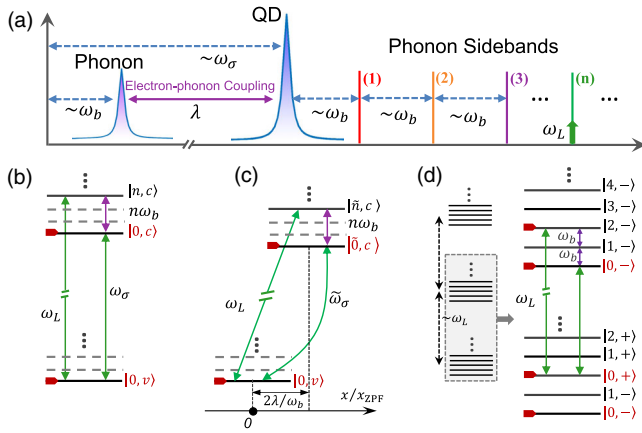


FIG. 1. (a) Scheme of the model and of the Stokes resonances in the frequency domain. The Stokes resonance is realized when a laser pumps the n th-order phonon sideband, which corresponds to (b) an ideal Raman process. For large electron-phonon coupling and pumping-laser intensity, the energy structure changes to that of the strong coupling regime $\lambda \sim \omega_b$ (c) and of the strong driving (Mollow) regime $\Omega \sim \omega_b$ (d). Panel (d) shows the case of two-phonon resonance, where the states $|n, +\rangle$ and $|n+2, -\rangle$ are degenerate. The dashed arrows in (d) represent the energy gap between two manifolds. Here, $x = (b + b^\dagger)/2$ is the position quadrature of the cavity mode, and x_{ZPF} is the corresponding zero-point fluctuation.

laser with frequency ω_L and amplitude Ω . The system Hamiltonian reads ($\hbar = 1$)

$$H = \omega_b b^\dagger b + \omega_\sigma \sigma^\dagger \sigma + \lambda \sigma^\dagger \sigma (b^\dagger + b) + \Omega (e^{i\omega_L t} \sigma + e^{-i\omega_L t} \sigma^\dagger), \quad (1)$$

where b^\dagger (b) is the creation (annihilation) operator of the phonon mode with resonance frequency ω_b and $\sigma = |v\rangle\langle c|$ (σ^\dagger) is the Pauli annihilation (creation) operator for the QD. Over a wide range of parameters, this system displays Stokes resonances associated with the periodic generation of n phonons in the acoustic cavity.

First, in the parameter regime $\Omega, \lambda \ll \omega_b$, where the influence on the energy structure of the electron-phonon coupling and driving laser can be ignored, the eigenstates of the system are given by the product states $|n, c/v\rangle$. As shown in Fig. 1(b), the ideal Stokes resonance between states $|0, v\rangle$, $|0, c\rangle$, and $|n, c\rangle$ is realized when the QD is driven at the frequency of the n th-order phonon sideband, i.e., $\Delta = \omega_\sigma - \omega_L = -n\omega_b$. Specifically, the QD flip is accompanied by the emission of n phonons into the acoustic cavity, induced by the electron-phonon interaction. One can obtain by perturbation theory the approximate Stokes transition rate between $|0, v\rangle$ and $|n, c\rangle$, leading to their super-Rabi oscillations at rate $\Omega_{\text{eff}}^{(n)} = \Omega(\lambda/\omega_b)^n / \sqrt{n!}$ [42].

Second, in the parameter regime $\lambda \sim \omega_b$, the strong electron-phonon coupling changes the energy structure, leading to different Stokes resonance conditions. This brings the system Hamiltonian to

$$H = \omega_b b^\dagger b + \tilde{\omega}_\sigma \sigma^\dagger \sigma + \Omega [\sigma^\dagger e^{-i\omega_L t + \frac{i}{\omega_b}(b^\dagger - b)} + \text{H.c.}] \quad (2)$$

through a displaced transformation $H \rightarrow DHD^\dagger$, where $D = \exp [(\lambda/\omega_b)\sigma^\dagger \sigma (b^\dagger - b)]$, with $\tilde{\omega}_\sigma = \omega_\sigma - \lambda^2/\omega_b$ the rescaled flip frequency of the QD. The reduced Hamiltonian is similar to that describing a trapped ion [44], with n -phonon Stokes resonances at $\Delta = \Delta_n(\lambda) = \lambda^2/\omega_b - n\omega_b$, as shown in Fig. 1(c), with the product state $|n, c\rangle$ being replaced by the displaced state $|\tilde{n}, c\rangle = D|n, c\rangle$. The n -phonon assisted Stokes transition rate becomes $\Omega_{\text{eff}}^{(n)} = \Omega e^{-\lambda^2/2\omega_b^2} (\lambda/\omega_b)^n / \sqrt{n!}$ [42].

Third, in the parameter regime $\Omega \sim \omega_b$, strong driving by the laser dresses the QD, and forms a Mollow ladder of manifolds, separated by the energy of the laser. As shown in Fig. 1(d), each manifold consists of many equidistant dressed states $|n, \pm\rangle$, which is different from the usual Mollow ladder in the optical cQED systems [45–48]. The dressed eigenstates of the QD are $|\pm\rangle = c_\pm |v\rangle \pm c_\mp |c\rangle$, where $c_\pm = \sqrt{2}\Omega/(\Delta^2 + 4\Omega^2 \pm \Delta\sqrt{\Delta^2 + 4\Omega^2})^{1/2}$, with corresponding eigenvalues $E_{|\pm\rangle} = \Delta/2 \pm \sqrt{\Delta^2 + 4\Omega^2}/2$. In this regime, n -phonon assisted Stokes resonances can still be realized. This occurs when the laser drives the

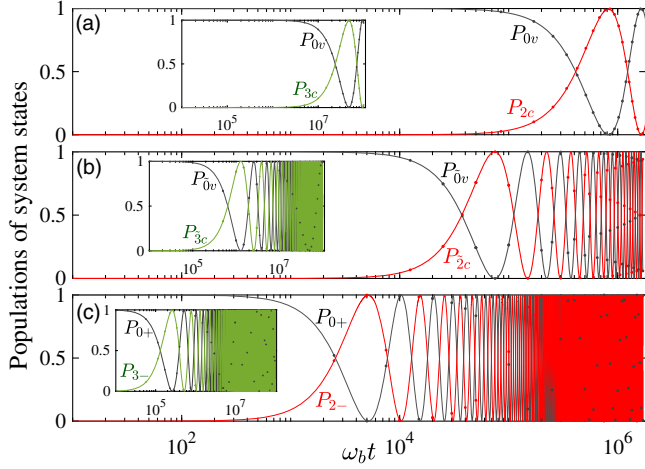


FIG. 2. Super-Rabi oscillations as seen through the population dynamics $P_{jk}(t) = |\langle j, k | \psi(t) \rangle|^2$ ($j = n, \tilde{n}$ and $k = c, v, +, -$) with $n = 2, 3$ corresponding to the main and inset parts, respectively. The solid lines and dots correspond to the exact numerical results and the analytical approximate solutions based on $\Omega_{\text{eff}}^{(n)}$ [42], respectively. System parameters are (a) $\lambda/\omega_b = 0.03$, $\Omega/\omega_b = 0.003$, (b) $\lambda/\omega_b = 0.1$, $\Omega/\omega_b = 0.003$, (c) $\lambda/\omega_b = 0.03$, $\Omega/\omega_b = 0.8$, corresponding to the regimes of Figs. 1(b), 1(c), and 1(d), respectively.

transition $|+\rangle \leftrightarrow |-\rangle$, at $\Delta = \Delta_n(\Omega) = -\sqrt{(n\omega_b)^2 - 4\Omega^2}$. The corresponding n -phonon transition rate is $\Omega_{\text{eff}}^{(n)} = (-1)^n \Omega (\lambda/\omega_b)^n [\prod_{k=1}^{n-1} (nc_-^2 - k)] / [(n-1)! \sqrt{n!}]$ [42].

We illustrate the above discussion in Fig. 2, where we present the essentially perfect super-Rabi oscillations $|0, v\rangle \leftrightarrow |n, c\rangle$, $|0, v\rangle \leftrightarrow |\tilde{n}, c\rangle$, and $|0, +\rangle \leftrightarrow |n, -\rangle$, in the absence of dissipation. This shows that, in these three different regimes, the two- and three-phonon states are periodically generated with high fidelity, thanks to the Stokes processes. This is the basic mechanism for the high-purity n -phonon bundle emission. Comparing Figs. 2(a) and 2(b), 2(c), one can see how increasing λ and Ω speeds up the super-Rabi oscillations, as is also clear from the approximate analytical solutions $\Omega_{\text{eff}}^{(n)}$ which can be seen to provide an excellent agreement in all three regimes. As shown below, higher frequencies of oscillations will yield higher n -phonon bundle emission rates.

N-phonon bundle emission.—The system dissipation has to be considered to trigger the emission. This is implemented with a Lindblad-type master equation $d\rho/dt = -i[H, \rho] + \kappa \mathcal{L}[b] + \gamma \mathcal{L}[\sigma] + \gamma_\phi \mathcal{L}[\sigma^\dagger \sigma]$ [49], where $\mathcal{L}[O] = (2O\rho O^\dagger - \rho O^\dagger O - O^\dagger O\rho)/2$, κ (γ) is the cavity (QD) decay rate, and γ_ϕ is the rate of pure dephasing of the QD. Dissipation transfers the above intracavity n -phonon states to bundles of strongly correlated phonons outside of the cavity. A first unambiguous evidence of strong correlations of the emitted phonons is given by the equal-time n th-order phonon correlation $g^{(n)} = \langle b^\dagger^n b^n \rangle / \langle b^\dagger b \rangle^n$. Figure 3(a) shows the sharp resonances to all orders of

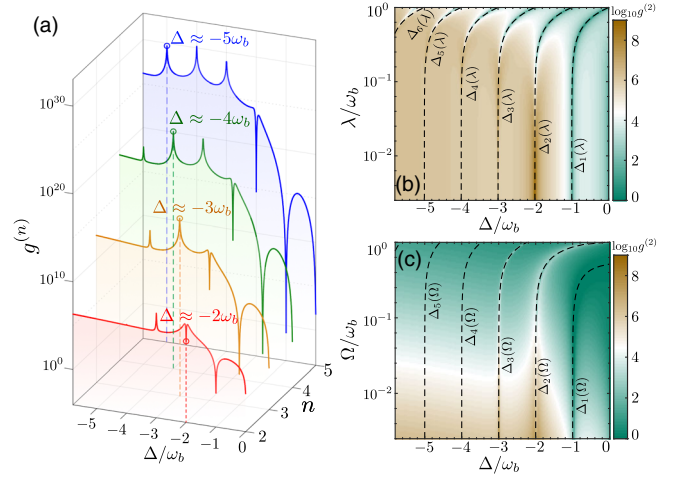


FIG. 3. (a) Equal-time n th-order correlation functions $g^{(n)}$ as a function of Δ/ω_b . (b)–(c) Correlation function $g^{(2)}$ for different λ/ω_b (b) and Ω/ω_b (c). The dashed lines indicate the n -phonon resonances $\Delta = -n\omega_b$, $\Delta = \Delta_n(\lambda)$, and $\Delta = \Delta_n(\Omega)$. System parameters are (a) $\lambda/\omega_b = 0.03$, $\Omega/\omega_b = 0.003$, (b) $\Omega/\omega_b = 0.003$, (c) $\lambda/\omega_b = 0.03$, and $\kappa/\omega_b = 0.002$, $\gamma/\omega_b = 0.0002$, and $\gamma_\phi/\omega_b = 0.0004$ for panels (a)–(c).

these correlation functions, clearly associated to the Stokes resonances $\Delta = -n\omega_b$ in the weak-coupling and low-driving regime. Note furthermore how a dip inside the bunching peak is observed right at the two-phonon resonance rather than a superbunching peak, as could be expected for multiphonon emission. The system enters a new regime of emission, namely, of strongly correlated bundles. As shown in Figs. 3(b) and 3(c), with increasing λ and Ω , the resonances in $g^{(2)}$ shift along the curves $\Delta = \Delta_n(\lambda)$ and $\Delta = \Delta_n(\Omega)$, respectively. Figure 3 also shows collectively that the frequency differences between the n and $(n+1)$ -phonon resonances ($\sim \omega_b$) are almost independent of the value of n , which is another clear signature of Stokes resonances (cf. Fig. 1). Interestingly, even for large n , the optimum pumping frequency to realize n -phonon emission can be well resolved under the conditions $\omega_b \gg \kappa, \gamma$, since the off-resonant phonon excitations are then strongly suppressed. This allows high purity n -phonon emission also for large n [42]. Since the order n of the bundle can be controlled simply by adjusting the frequency of the pumping laser, our proposal realizes a versatile optically controlled multiphonon source.

The correlation functions $g^{(n)}$ do not guarantee an actual n -phonon emission, although it reveals strong phonon correlations at the Stokes resonances. This failure is manifest from the resonant dip sitting on the superbunching peak when the system enters the pure-bundle emission regime, in which case $g^{(n)}$ breaks down as single phonons lose meaning and correlations between bundles themselves should be considered instead, which is achieved through generalized correlation functions $g_m^{(n)}$ [42]. They show that

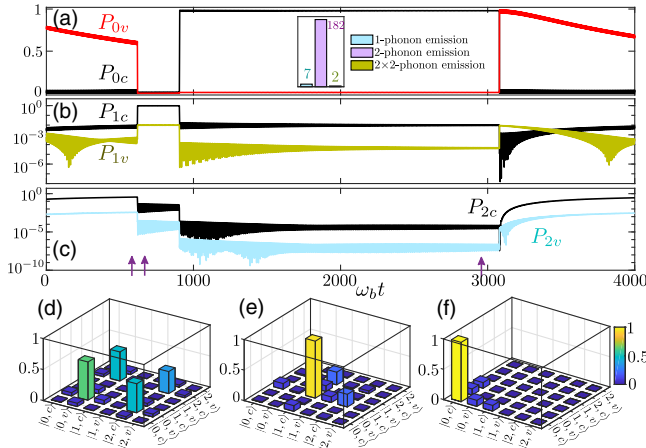


FIG. 4. (a)–(c) Small fraction of a quantum trajectory in the regime of two-phonon emission. The inset bar graphs show the total number of single-, two- and $2n$ -phonon ($n = 2$) clicks over 25 quantum trajectories. (d)–(f) Full density matrices of the system at the times indicated with purple arrows in the trajectory, showing the cascade-emission process. System parameters are $\lambda/\omega_b = 0.1$, $\Omega/\omega_b = 0.2$, $\kappa/\omega_b = 0.002$, $\gamma/\omega_b = 0.0002$, and $\gamma_\phi/\omega_b = 0.0004$, satisfying the regime around the sweet point $\kappa \approx 10\Omega_{\text{eff}}^{(2)}$ [42].

bundles can be antibunched (n -phonon guns), uncorrelated (n -phonon laser), or bunched (thermal states of bundles). To prove n -phonon emission, we turn to Monte Carlo simulations [4]. In this way, one can follow individual trajectories of the system and record phonon clicks whenever the system undergoes a quantum jump. Figures 4(a)–4(c) show a tiny fraction of a quantum trajectory during a two-phonon emission (a larger fraction is shown in Ref. [42]) under the Stokes resonance. In this segment, the two-phonon state is initially occupied with a probability greater than 30%, while the probability for the one-phonon state is smaller than 0.1%. When the system undergoes a quantum collapse of its wave function triggered by dissipation, it is thus exceedingly more likely to realize the two-phonon state. This occurs with the emission of a first phonon that leaves the system in the one-phonon state with almost unit probability, also highly likely to be emitted during the cavity lifetime, and thus shortly after the first phonon, completing the two-phonon bundle emission. As a result, the system has emitted two strongly-correlated phonons in a very short temporal window. The system that is left in the phonon-vacuum and the excited state of the QD can then resume the cycle after a direct *photon* emission $|0, c\rangle \rightarrow |0, v\rangle$ from the QD flip. In the next cycle, the system undergoes the same cascade emission of phonon pair, each accompanied by a single *photon* emission, which can be used for heralding purposes (e.g., with a delay line). The emitted single photon does not disturb the phonon bundle thanks to their different nature. The inset bar graphs

in Fig. 4(a) show that the overall two-phonon emission is the largely dominant process in this regime, chosen as the optimal two-phonon resonant condition including the influence of the electron-phonon coupling and of the driving laser. It also shows that the undesired $2n$ -phonon bundle emission ($n = 2$) with a probability close to 1% is negligible [42]. This corresponds to two-phonon emission rates as high as $\approx 1.1 \times 10^9 / s$ when $\omega_b/2\pi = 1$ THz, for the chosen values of Ω and λ . The emitted n -phonon bundle has an intrinsic and characteristic temporal structure as a result of its dynamical character, which corresponds to the spontaneous emission of a Fock state [4]. As shown in Figs. 4(d)–4(f), initially, the system is essentially in a quantum superposition of the states $|0, v\rangle$ and $|n, c\rangle$. It then experiences a rapid cascade emission through the Fock states $|n_i\rangle$ ($0 \leq n_i \leq n$) in a short time window. Here, $n = 2$ and $n_i = 1$ show the cascaded two-phonon emission (other cases are shown in Ref. [42]).

Discussions of purity and experimental feasibility.—In an actual system, or with exact numerical simulations, there is always a contamination of the n -phonon emission by other processes, even when the system is driven at a perfect n -phonon assisted Stokes resonance. In our case, this comes chiefly from off-resonant m -phonon emission ($m \neq n$). We thus calculate numerically the purity Π_n of n -phonon emission, which is defined as $\Pi_n = \bar{P}_n / \sum_{n_i=1}^n \bar{P}_{n_i}$ [4,50], where \bar{P}_{n_i} is obtained by sampling the phonon-state populations in time-windows T chosen at random times for numerous trajectories of the Monte Carlo simulation, until enough statistics is acquired to ensure convergence of the probability distribution. Figure 5 shows that two- and three-phonon emissions with high purities (> 95%) can be realized in a wide range of parameters for κ/ω_b and λ/ω_b , under the Stokes conditions. The effect of off-resonant phonon emission on the purity is more notable for larger cavity decay rates. Especially, as n increases, this

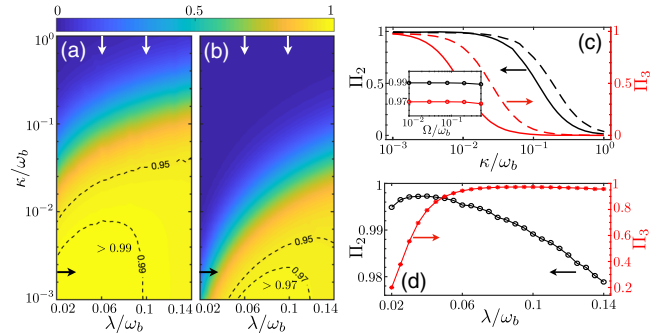


FIG. 5. Purities of (a) two-phonon and (b) three-phonon emissions vs λ/ω_b and κ/ω_b when $\Omega/\omega_b = 0.2$. (c) Vertical cuts of the purity along the arrows in (a) and (b). The solid and dashed lines correspond to $\lambda/\omega_b = 0.06$ and $\lambda/\omega_b = 0.1$, respectively. (d) Horizontal cuts of the purity along the arrows in (a) and (b). Inset: Purities vs Ω/ω_b when $\lambda/\omega_b = 0.1$ and $\kappa/\omega_b = 0.002$. System parameters are $\gamma/\omega_b = 0.0002$ and $\gamma_\phi/\omega_b = 0.0004$.

effect is more obvious due to the occurrence of more off-resonant transitions. Moreover, increasing λ/ω_b can enhance (decrease) the three-phonon (two-phonon) emission purity by enhancing the high-order phonon sideband processes. More interestingly, the inset of Fig. 5(c) shows that high purities ($> 97\%$) are robust with the driving amplitude Ω , since increasing Ω cannot extremely enhance the effective Rabi frequency for this regime. Note that throughout, we have considered realistic values of pure dephasing for the QD. Its effect is basically negligible on the purity since bundles are quickly emitted in a fast cascaded emission following the wave function collapse, prior to which the cavity is in the vacuum and shielded from QD dephasing [42].

Regarding experimental implementations, while we have considered here a semiconductor system with a quantum dot coupled to a THz acoustic nanocavity, our proposal is not limited to this particular architecture and could be implemented or adapted in a variety of platforms. For our specific design, the theoretical model predicts that the current technology [12–15] should already be able to deliver around 99% two-phonon and 97% three-phonon emission ($\omega_b/2\pi = 1$ THz, $\omega_\sigma/2\pi = 100$ THz, $\Omega/2\pi = 0.2$ THz, $\lambda/2\pi = 0.1$ THz, $\kappa/2\pi = 2$ GHz, $\gamma/2\pi = 0.2$ GHz, and $\gamma_\phi/2\pi = 0.4$ GHz). A direct observation of our phenomenon could be made with a nanocalorimeter, where phonons are converted into electrons by interactions between the nanocavity and the electron gas (transducer), thus allowing phonon counting and other types of statistical processing [51,52] with well-controlled electronics.

Conclusions—We have proposed an efficient method for producing n -phonon bundle emission based on the Stokes process. The bundle emission with high purity ($> 97\%$) is obtained over a wide range of parameters. The purity of the n -phonon emission depends on the cavity decay and the electron-phonon coupling strength, and is robust with the strength of the pumping laser. The proposal is easily tunable simply by adjusting the frequency of the pumping laser, allowing essentially pure two- and three-phonon emissions with the currently available technology. Our work can also be extended to periodic bundle emission of phonons by using the collective properties of a comb-shaped ensemble of QDs [53], which is attractive for applications that are clocked in periodic time intervals.

We thank E. del Valle and C. S. Muñoz for discussions. We gratefully acknowledge use of the open source Python numerical packages Numpy, Scipy, and QuTiP [54]. This work is supported by the National Science Foundation of China (Grants No. 11822502, No. 11974125, and No. 11875029), the National Key Research and Development Program of China Grant No. 2016YFA0301203. F. N. is supported in part by the MURI Center for Dynamic Magneto-Optics via the Air

Force Office of Scientific Research (AFOSR) (FA9550-14-1-0040), Army Research Office (ARO) (Grant No. W911NF-18-1-0358), Asian Office of Aerospace Research and Development (AOARD) (Grant No. FA2386-18-1-4045), Japan Science and Technology Agency (JST) (via the Q-LEAP program, and the CREST Grant No. JPMJCR1676), Japan Society for the Promotion of Science (JSPS) (JSPS-RFBR Grant No. 17-52-50023, and JSPS-FWO Grant No. VS.059.18N), the RIKEN-AIST Challenge Research Fund, and the NTT Physics and Informatics Labs.

*xinyoulu@hust.edu.cn

†yingwu2@126.com

- [1] A. Kubanek, A. Ourjoumtsev, I. Schuster, M. Koch, P. W. H. Pinkse, K. Murr, and G. Rempe, Two-Photon Gateway in One-Atom Cavity Quantum Electrodynamics, *Phys. Rev. Lett.* **101**, 203602 (2008).
- [2] Y. Ota, S. Iwamoto, N. Kumagai, and Y. Arakawa, Spontaneous Two-Photon Emission from a Single Quantum Dot, *Phys. Rev. Lett.* **107**, 233602 (2011).
- [3] A. Gonzalez-Tudela, F. P. Laussy, C. Tejedor, M. J. Hartmann, and E. del Valle, Two-photon spectra of quantum emitters, *New J. Phys.* **15**, 033036 (2013).
- [4] C. S. Muñoz, E. del Valle, A. G. Tudela, K. Müller, S. Lichtmannecker, M. Kaniber, C. Tejedor, J. Finley, and F. P. Laussy, Emitters of N -photon bundles, *Nat. Photonics* **8**, 550 (2014).
- [5] Y. Chang, A. González-Tudela, C. S. Muñoz, C. Navarrete-Benlloch, and T. Shi, Deterministic Down-Converter and Continuous Photon-Pair Source Within the Bad-Cavity Limit, *Phys. Rev. Lett.* **117**, 203602 (2016).
- [6] A. F. Kockum, A. Miranowicz, V. Macrì, S. Savasta, and F. Nori, Deterministic quantum nonlinear optics with single atoms and virtual photons, *Phys. Rev. A* **95**, 063849 (2017).
- [7] D. J. Gauthier, Q. L. Wu, S. E. Morin, and T. W. Mossberg, Realization of a Continuous-Wave, Two-Photon Optical Laser, *Phys. Rev. Lett.* **68**, 464 (1992).
- [8] M. D'Angelo, M. V. Chekhova, and Y. Shih, Two-Photon Diffraction and Quantum Lithography, *Phys. Rev. Lett.* **87**, 013602 (2001).
- [9] I. Afek, O. Ambar, and Y. Silberberg, High-NOON states by mixing quantum and classical light, *Science* **328**, 879 (2010).
- [10] M. V. Gustafsson, T. Aref, A. F. Kockum, M. K. Ekström, G. Johansson, and P. Delsing, Propagating phonons coupled to an artificial atom, *Science* **346**, 207 (2014).
- [11] M. C. Kuzyk and H. L. Wang, Scaling Phononic Quantum Networks of Solid-State Spins with Closed Mechanical Subsystems, *Phys. Rev. X* **8**, 041027 (2018).
- [12] P. Borri, W. Langbein, S. Schneider, and U. Woggon, Ultralong Dephasing Time in InGaAs Quantum Dots, *Phys. Rev. Lett.* **87**, 157401 (2001).
- [13] E. M. Weig, R. H. Blick, T. Brandes, J. Kirschbaum, W. Wegscheider, M. Bichler, and J. P. Kotthaus, Single-Electron-Phonon Interaction in a Suspended Quantum Dot Phonon Cavity, *Phys. Rev. Lett.* **92**, 046804 (2004).

- [14] G. Rozas, M. F. P. Winter, B. Jusserand, A. Fainstein, B. Perrin, E. Semenova, and A. Lemaître, Lifetime of THz Acoustic Nanocavity Modes, *Phys. Rev. Lett.* **102**, 015502 (2009).
- [15] E. Stock, M.-R. Dachner, T. Warming, A. Schliwa, A. Lochmann, A. Hoffmann, A. I. Toropov, A. K. Bakarov, I. A. Derebezon, M. Richter, V. A. Haisler, A. Knorr, and D. Bimberg, Acoustic and optical phonon scattering in a single In(Ga)As quantum dot, *Phys. Rev. B* **83**, 041304 (2011).
- [16] Ö.O. Soykal, R. Ruskov, and C. Tahan, Sound-Based Analogue of Cavity Quantum Electrodynamics in Silicon, *Phys. Rev. Lett.* **107**, 235502 (2011).
- [17] A. Fainstein, N. D. Lanzillotti-Kimura, B. Jusserand, and B. Perrin, Strong Optical-Mechanical Coupling in a Vertical GaAs/AlAs Microcavity for Subterahertz Phonons and Near-Infrared Light, *Phys. Rev. Lett.* **110**, 037403 (2013).
- [18] Y. T. Xu, W. Fu, C.-I. Zou, Z. Shen, and H. X. Tang, High quality factor surface Fabry-Perot cavity of acoustic waves, *Appl. Phys. Lett.* **112**, 073505 (2018).
- [19] P. Kharela, Y. W. Chu, M. Power, W. H. Renninger, R. J. Schoelkopf, and P. T. Rakich, Ultra-high-Q phononic resonators on-chip at cryogenic temperatures, *APL Photonics* **3**, 066101 (2018).
- [20] J. Kabuss, A. Carmele, T. Brandes, and A. Knorr, Optically Driven Quantum Dots as Source of Coherent Cavity Phonons: A Proposal for a Phonon Laser Scheme, *Phys. Rev. Lett.* **109**, 054301 (2012).
- [21] W. Maryam, A. V. Akimov, R. P. Campion, and A. J. Kent, Dynamics of a vertical cavity quantum cascade phonon laser structure, *Nat. Commun.* **4**, 2184 (2013).
- [22] H. X. Han, B. W. Li, S. Volz, and Y. A. Kosevich, Ultra-compact Interference Phonon Nanocapacitor for Storage and Lasing of Coherent Terahertz Lattice Waves, *Phys. Rev. Lett.* **114**, 145501 (2015).
- [23] M.-A. Lemonde, S. Meesala, A. Sipahigil, M. J. A. Schuetz, M. D. Lukin, M. Loncar, and P. Rabl, Phonon Networks with Silicon-Vacancy Centers in Diamond Waveguides, *Phys. Rev. Lett.* **120**, 213603 (2018).
- [24] G. Calajó, M. J. A. Schuetz, H. Pichler, M. D. Lukin, P. Schneeweiss, J. Volz, and P. Rabl, Quantum acousto-optic control of light-matter interactions in nanophotonic networks, *Phys. Rev. A* **99**, 053852 (2019).
- [25] T. R. Hartke, Y.-Y. Liu, M. J. Gullans, and J. R. Petta, Microwave Detection of Electron-Phonon Interactions in a Cavity-Coupled Double Quantum Dot, *Phys. Rev. Lett.* **120**, 097701 (2018).
- [26] M. J. Gullans, J. M. Taylor, and J. R. Petta, Probing electron-phonon interactions in the charge-photon dynamics of cavity-coupled double quantum dots, *Phys. Rev. B* **97**, 035305 (2018).
- [27] M. J. A. Schuetz, E. M. Kessler, G. Giedke, L. M. K. Vandersypen, M. D. Lukin, and J. I. Cirac, Universal Quantum Transducers Based on Surface Acoustic Waves, *Phys. Rev. X* **5**, 031031 (2015).
- [28] R. Manenti, A. F. Kockum, A. Patterson, T. Behrle, J. Rahamim, G. Tancredi, F. Nori, and P. J. Leek, Circuit quantum acoustodynamics with surface acoustic waves, *Nat. Commun.* **8**, 975 (2017).
- [29] Y. W. Chu, P. Kharel, T. Yoon, L. Frunzio, P. T. Rakich, and R. J. Schoelkopf, Creation and control of multi-phonon Fock states in a bulk acoustic-wave resonator, *Nature (London)* **563**, 666 (2018).
- [30] K. J. Satzinger, Y. P. Zhong, H.-S. Chang, G. A. Peairs, A. Bienfait, M.-H. Chou, A. Y. Cleland, C. R. Conner, É. Dumur, J. Grebel, I. Gutierrez, B. H. November, R. G. Povey, S. J. Whiteley, D. D. Awschalom, D. I. Schuster, and A. N. Cleland, Quantum control of surface acoustic-wave phonons, *Nature (London)* **563**, 661 (2018).
- [31] K. Toyoda, R. Hiji, A. Noguchi, and S. Urabe, Hong-Ou-Mandel interference of two phonons in trapped ions, *Nature (London)* **527**, 74 (2015).
- [32] J. H. Zhang, M. Um, D. S. Lv, J.-N. Zhang, L.-M. Duan, and K. Kim, NOON States of Nine Quantized Vibrations in Two Radial Modes of a Trapped Ion, *Phys. Rev. Lett.* **121**, 160502 (2018).
- [33] X. Y. Chu, X. Honga, P. Zou, J. Men, and Y. C. Liu, Ultrasensitive protein detection in terms of multiphonon resonance Raman scattering in ZnS nanocrystals, *Appl. Phys. Lett.* **98**, 253703 (2011).
- [34] D. V. Strekalov, A bundle of photons, *Nat. Photonics* **8**, 500 (2014).
- [35] S. J. M. Habraken, K. Stannigel, M. D. Lukin, P. Zoller, and P. Rabl, Continuous mode cooling and phonon routers for phononic quantum networks, *New J. Phys.* **14**, 115004 (2012).
- [36] A. Bienfait, K. J. Satzinger, Y. P. Zhong, H.-S. Chang, M.-H. Chou, C. R. Conner, É. Dumur, J. Grebel, G. A. Peairs, R. G. Povey, and A. N. Cleland, Phonon-mediated quantum state transfer and remote qubit entanglement, *Science* **364**, 368 (2019).
- [37] V. Balić, D. A. Braje, P. Kolchin, G. Y. Yin, and S. E. Harris, Generation of Paired Photons with Controllable Waveforms, *Phys. Rev. Lett.* **94**, 183601 (2005).
- [38] M. D. Eisaman, A. André, F. Massou, M. Fleischhauer, A. S. Zibrov, and M. D. Lukin, Electromagnetically induced transparency with tunable single-photon pulses, *Nature (London)* **438**, 837 (2005).
- [39] M. Aspelmeyer, T. J. Kippenberg, and F. Marquardt, Cavity optomechanics, *Rev. Mod. Phys.* **86**, 1391 (2014).
- [40] L. Droenner, N. L. Naumann, J. Kabuss, and A. Carmele, Collective enhancements in many-emitter phonon lasing, *Phys. Rev. A* **96**, 043805 (2017).
- [41] T. P. Devereaux and R. Hackl, Inelastic light scattering from correlated electrons, *Rev. Mod. Phys.* **79**, 175 (2007).
- [42] See Supplemental Material at <http://link.aps.org/supplemental/10.1103/PhysRevLett.124.053601> for the analytical calculation of the super-Rabi oscillation frequencies, purity of higher-order emission, effect of pure dephasing, optimization of bundle emission, and quantum correlation of n -phonon bundle, which includes Ref. [43].
- [43] K. K. W. Ma and C. K. Law, Three-photon resonance and adiabatic passage in the large-detuning Rabi model, *Phys. Rev. A* **92**, 023842 (2015).
- [44] C. A. Blockley, D. F. Walls, and H. Risken, Quantum collapses and revivals in a quantized trap, *Europhys. Lett.* **17**, 509 (1992).

- [45] B. R. Mollow, Power spectrum of light scattered by two-level systems, *Phys. Rev.* **188**, 1969 (1969).
- [46] C. N. Cohen-Tannoudji and S. Reynaud, Dressed-atom description of resonance fluorescence and absorption spectra of a multi-level atom in an intense laser beam, *J. Phys. B* **10**, 345 (1977).
- [47] J. Zakrzewski, M. Lewenstein, and T. W. Mossberg, Theory of dressed-state lasers. I. Effective Hamiltonians and stability properties, *Phys. Rev. A* **44**, 7717 (1991).
- [48] J. C. L. Carreño, E. del Valle, and F. P. Laussy, Photon correlations from the Mollow Triplet, *Laser Photonics Rev.* **11**, 1700090 (2017).
- [49] R. J. Glauber, The quantum theory of optical coherence, *Phys. Rev.* **130**, 2529 (1963).
- [50] C. S. Muñoz, F. P. Laussy, E. del Valle, C. Tejedor, and A. González-Tudela, Filtering multiphoton emission from state-of-the-art cavity quantum electrodynamics, *Optica* **5**, 14 (2018).
- [51] M. L. Roukes, Yoctocalorimetry: Phonon counting in nanostructures, *Physica (Amsterdam)* **263B**, 1 (1999).
- [52] W. D. Oliver, J. Kim, R. C. Liu, and Y. Yamamoto, Hanbury Brown and Twiss-Type Experiment with electrons, *Science* **284**, 299 (1999).
- [53] H. S. Dhar, M. Zens, D. O. Krimer, and S. Rotter, Variational Renormalization Group for Dissipative Spin-Cavity Systems: Periodic Pulses of Nonclassical Photons from Mesoscopic Spin Ensembles, *Phys. Rev. Lett.* **121**, 133601 (2018).
- [54] J. R. Johansson, P. D. Nation, and F. Nori, QuTiP: An open-source Python framework for the dynamics of open quantum systems, *Comput. Phys. Commun.* **183**, 1760 (2012).